Sinusoidal vs. Square-Wave Current Supply of PM Brushless DC Drives: a Convenience Analysis

This article has been accepted for publication in a future issue of this journal, but has not been fully edited. Content may change prior to final publication. Citation information: DOI 10.1109/TIE.2015.2455518, IEEE Transactions on Industrial Electronics

Sinusoidal vs. Square-Wave Current Supply of PM Brushless DC Drives: a Convenience Analysis

Manuele Bertoluzzo, Giuseppe Buja, *Life Fellow, IEEE*, Ritesh Kumar Keshri, *Member, IEEE* and Roberto Menis, *Member, IEEE*

***Abstract*—PM BLDC drives are utilized in a variety of applications because of their inherent features, and would be even more utilized if their torque performance could be improved. Indeed, when supplied with square-wave currents, the torque-speed characteristic undergoes a drop at high speeds and a significant torque ripple arises at both low and high speeds due to the commutation phenomena. In this paper, the sinusoidal current supply of the PM BLDC motors is investigated in depth, and an analytical formulation of the torque-speed characteristic, the torque ripple and the base speed for such a supply are found. Based on the resulting equations, a thorough convenience analysis of the sinusoidal current supply is carried out with respect the square-wave one in presence of the commutation phenomena, hereafter termed the real square-wave current supply. Simulation and experimental tests for a study case are given to corroborate the theoretical results. Generation of the sinusoidal current references using Hall sensors is also discussed**

***Index Terms* — PM BLDC drives; torque-speed characteristic; torque ripple; sinusoidal current supply; square-wave current supply.**

NOMENCLATURE

a,b,c	Motor phases
e_j	Instantaneous motor phase back emf ($j = a,b,c$)
E	Magnitude of the flat-top portion of e_j
i_j	Instantaneous phase current ($j = a,b,c$)
I	Magnitude of the square-wave phase currents
I_s	Peak magnitude of the sinusoidal phase currents
$I_{d,q}$	Magnitude of the d,q current components
$k_\Phi=k\Phi$	Motor constant, where k is the armature constant and Φ is the flux
L	Inclusive inductance of a motor phase
R	Resistance of a motor phase
p	Pole pairs
p_i,	Instantaneous electric power
P	Active electric power
TR	Torque ripple
v_{jn}	Instantaneous phase voltage ($j = a,b,c$)
V_N	Nominal motor voltage
V_L	Peak magnitude of the voltage drop across L
τ	Instantaneous motor torque
T	Average motor torque
θ	Angular phase
Ω	Motor speed

Subscripts B, N, pu denote base, nominal and per-unit quantities, respectively. Subscripts *s* and *q* denote quantities relevant to the sinusoidal and real square-wave current supply, respectively.

Manuscript received February 2, 2015; revised May 11, 2015; accepted June 16, 2015.

G. Buja and M. Bertoluzzo are with the Department of Industrial Engineering, University of Padova, 35131 Padova, Italy (e-mail: giuseppe.buja@unipd.it; manuele.bertoluzzo@unipd.it).

R. K. Keshri is with the Department of Electrical and Electronics Engineering, Birla Institute of Technology, Mesra 834 004, India (e-mail: riteshkeshri@ieee.org).

R. Menis is with the Department of Engineering and Architecture, University of Trieste, 34127 Trieste, Italy (e-mail: menis@units.it).

I. INTRODUCTION

Permanent-magnet (PM) brushless (BL) motors are characterized by efficiencies and power densities higher than brushed DC and induction motors of the same size [1]. To change the operating speed, the PM BL motors are fed by inverters and the resulting setups constitute a drive. According to the shape of the motor back-emf, which can be trapezoidal or sinusoidal, the PM BL drives are termed PM BL direct current (BLDC) or PM BL alternating current (BLAC) drives, respectively [2].

PM BL drives are utilized in a variety of industrial and civil equipment, ranging from machine tools to home appliances and electrical traction [3], [4]. In general, PM BLAC drives are preferred for their constant torque-speed characteristic and smooth instantaneous torque, whereas PM BLDC drives are preferred for their robust structure and inexpensive sensor arrangement [5]. As a return, the torque-speed characteristic of the PM BLDC drives drops at high speeds and their instantaneous torque is affected by a significant ripple at both low and high speeds [6].

Actually, for the PM BLDC drives to exhibit a constant speed-torque characteristic up to the base speed and a ripple-free instantaneous torque, two conditions must be met, namely i) supply of the motor phases with square-wave currents having steeply edges, i.e. with currents having an ideal square waveform, and ii) synchronization of the edges of the currents to the flat portions of the back-emfs. While synchronization is easily achieved by means of three Hall sensors located on the stator, the ideal square waveform can not be achieved. This because the phase inductances of the motor slow down both the rise and the fall of the phase currents, originating the commutation phenomena. The ensuing supply is hereafter termed real square-wave current supply. Consequently, the torque performance of the PM BLDC drives is impaired in terms of capability of both developing the nominal torque up to the base speed and

This article has been accepted for publication in a future issue of this journal, but has not been fully edited. Content may change prior to final publication. Citation information: DOI 10.1109/TIE.2015.2455518, IEEE Transactions on Industrial Electronics

exhibiting a smooth instantaneous torque. Torque performance impairment due the commutation phenomena has been discussed in many papers [7]-[9]. To cope with such an impairment, a number of control techniques of the phase currents during the commutations have been proposed [10]-[16] but they either eliminate partially the above-mentioned shortcomings or make the drive control somewhat complex. For instance, paper [14] minimizes the torque ripple by a selective elimination of torque harmonics achieved through the supply of the motor phases with a sinusoidal-like current waveform, distorted with injection of harmonics of proper amplitude and phase. Papers [15] and [16] remove torque ripple in two steps: the off-line detection of the profile of the back-emfs of the motor and the on-line manipulation of the instantaneous value of the phase currents, executed by accounting of the detected back-emfs, for the developed torque to be constant.

This paper analyzes the convenience of supplying the PM BLDC motors with pure sinusoidal currents to mitigate the torque performance impairment due to the real square-wave current supply. Although other papers [17]-[19] have dealt with the sinusoidal supply of the PM BLDC motors, they have mostly faced applicative aspects rather than expatiating on a theoretic analysis on the achievable torque performance or on a comparison of the performance against that one of the real square-wave current supply. Indeed, paper [17] has redesigned the PM BLDC motor to modify the back-emf waveform with the aim of reducing the torque ripple when the motor is supplied with sinusoidal currents. Paper [18] has studied the behavior of a PM BLDC motor supplied with either sinusoidal or square-wave currents, whereby the study is executed by simulation. Paper [19] has proposed to supply a PM BLDC motor with voltages of sinusoidal waveform but this supply gives rise to currents that, besides the fundamental one, contain harmonics whose interaction with the harmonics of the trapezoidal phase back-emfs still produces a torque ripple even if by a different mechanism.

Unlike [17]-[19], this paper i) provides an analytical formulation of the torque-speed characteristic, the torque ripple and the base speed of a PM BLDC drive with sinusoidal current supply, ii) compares the torque performance of the PM BLDC drive with the ones obtained when the drive is supplied with real square-wave current supply. Comparison executed on the basis of the analytical results is supported by experimental measurements, and shows that the sinusoidal current supply outperforms the real square-wave one almost everywhere over the speed range. Experiments refer to the study case of a commercial PM BLDC drive the data of which are reported in the Appendix Section.

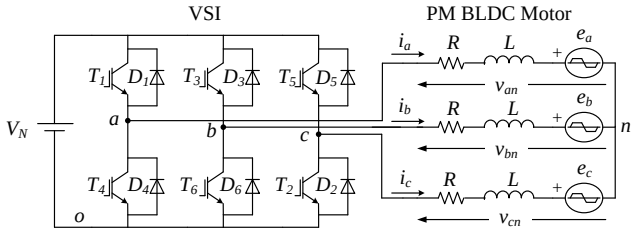

Fig.1. Circuital scheme of PM BLDC drive.

II. PM BLDC DRIVE

Fig.1 shows the scheme of a PM BLDC drive. The motor has no neutral connection and is represented in Fig.1 by its equivalent circuit. To fully exploit the motor capabilities, the voltage of the DC source feeding the voltage source inverter (VSI) is set at the nominal motor voltage V_N.

A. *Ideal square-wave current supply*

The trapezoidal back-emfs and the ideal square-wave currents supplying the motor phases are traced in Fig.2, where θ_e is the angular phase in electrical radians, E is the flat-top value of the back-emfs and I is the magnitude of the square-wave of current. The current flows in a phase during a supply period for two intervals the length of which are $2\pi/3$.

The subsequent analysis is carried out in steady-state under constant motor speed Ω. Then the supply angular frequency Ω_e and the angular phase are expressed as

$$\Omega_e = p\Omega \ , \quad \theta_e = \Omega_e t \tag{1}$$

The conventional nominal speed Ω_N and no-load speed Ω_0 of the motor are co-related with the nominal motor voltage V_N by

$$\Omega_N = \frac{V_N - 2RI_N}{2k_\Phi}, \quad \Omega_O = \frac{V_N}{2k_\Phi} \tag{2}$$

In the first equation of (2), I_N is the nominal motor current, and V_N - $2RI_N$ is equal to $2E_N$, where E_N is the nominal magnitude of E, given by

$$E_N = k_\Phi \Omega_N \tag{3}$$

The instantaneous motor torque τ can be expressed as

$$\tau = \frac{p_i}{\Omega} \tag{4}$$

where p_i is the instantaneous electric power converted into mechanical form and is expressed as

$$p_i = e_a i_a + e_b i_b + e_c i_c \tag{5}$$

By definition, the average motor torque is the average value of the instantaneous torque over the supply period. Here and later on, it is simply termed motor torque. For the ideal

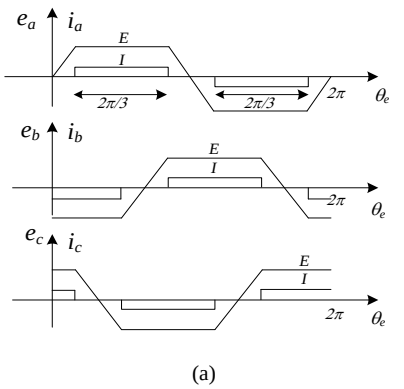

(a)

Fig.2. Phase back-emfs and ideal square-wave current supply.

This article has been accepted for publication in a future issue of this journal, but has not been fully edited. Content may change prior to final publication. Citation information: DOI 10.1109/TIE.2015.2455518, IEEE Transactions on Industrial Electronics

square-wave current supply, the power p_i is constant, equal to the active electric power P converted in mechanical form, and given by $2EI$. By (4), also the instantaneous motor torque is constant. In nominal conditions, the active electric power is equal to $2E_N I_N$ and the nominal torque to

$$T_N = 2k_\Phi I_N \tag{6}$$

B. Convenience analysis premises

In practice, injection and removal of square-wave currents into and from the motor phases are impeded by the phase inductances (and the limited DC source voltage), giving rise to the commutation phenomena. Then the currents fail to maintain the square waveform and, furthermore, even the waveform of the non-commutating current is altered during the commutations. As a result, the instantaneous torque developed by the motor is subjected to excursions that deviate its value from the requested one, causing the torque ripple. Torque ripple is more conspicuous at both low and high speeds. At low speeds because the back-emf is somewhat weak to remove quickly the current from the phase at the end of the conduction interval so that the current falling edge is slowed down; at high speeds because the back-emf is somewhat remarkable to oppose the DC voltage source in injecting the current into the phase at the beginning of the conduction interval so that the current rising edge is slowed down. At low speeds, the torque ripple does not affect too much the motor torque that hence takes the value exhibited with the ideal square-wave current supply. Instead, at high speeds the torque ripple produces a drop of the motor torque that is more and more noticeable as the speed increases.

It appears evident since now that the sinusoidal current supply reduces the voltage requirements across the phase inductance on account of the softer change of the current shape. Moreover, the sinusoidal current supply is expected to be maintained in an equal way at both low and high speeds, thus avoiding any difference in both the instantaneous and average values of the motor torque within the speed range.

Analysis of the sinusoidal current supply is carried out by assuming:

i) equal values for the peak voltage applied across the motor phases for both the sinusoidal and the real square-wave supply,

ii) equal values for the rms value of current flowing into the motor phases in nominal conditions for both the sinusoidal and the real square-wave supply. By approximating the rms value of the phase current for the real square-wave supply to that one of the ideal square-wave, given by $\sqrt{2/3}\,I_N$, and by equating it to the rms value of the phase current for the sinusoidal supply, given by $1/\sqrt{2}I_{s,N}$ where $I_{s,N}$ is its peak magnitude, one obtains

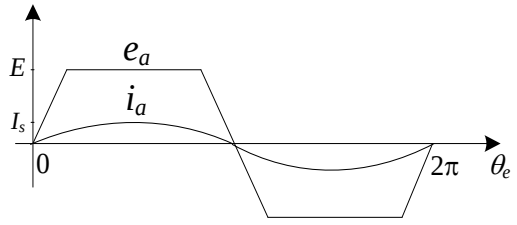

Fig.3. Sinusoidal current supply.

$$\sqrt{\frac{2}{3}}I_N = \frac{1}{\sqrt{2}}I_{s,N} \tag{7}$$

From (7), $I_{s,N}$ must be equal to

$$I_{s,N} = \frac{2}{\sqrt{3}}I_N \tag{8}$$

iii) a negligible voltage drop on the phase resistances.

Moreover, the analysis expresses speed and torque quantities in per-unit of Ω_0 and T_N as defined in (2) and (6), respectively.

III. Sinusoidal Current Supply

With the sinusoidal current supply, the phase currents are kept in phase with the fundamental components of the back-emfs to maximize the motor torque-per-ampere. Back-emf and current of the phase *a* are traced in Fig.3. Equation of the current for the phase *a* in nominal conditions is then

$$i_a = I_{s,N}\,sin(\theta_e) \tag{9}$$

Equations of the currents for the phases *b* and *c* can be readily obtained by shifting (9) of $-2\pi/3$ and $-4\pi/3$, respectively.

A. Motor torque

The active electric power P_s that the motor converts into mechanical form is equal to three times the product of the rms value $E_{1,rms}$ of the fundamental component of the back-emf by the rms value of the sinusoidal current supply, i.e. to $3\,E_{1,rms}\,I_{s,rms}$. The peak magnitude E_1 of the fundamental component of the back-emf is the Fourier coefficient of order 1 of $e_a(\theta_e)$; by exploiting the quarter-wave symmetry of the back-emf waveform, it is

$$E_1 = \frac{4}{\pi}\left(\frac{6E}{\pi}\int_0^{\pi/6}\theta_e\,sin(\theta_e)d\theta_e + E\int_{\pi/6}^{\pi/2}sin(\theta_e)d\theta_e\right) = \frac{12}{\pi^2}E \tag{10}$$

Then P_s, calculated in nominal conditions and expressed as a function of the peak value of the sinusoidal current, is equal to

$$P_{s,N} = \frac{18}{\pi^2}E_N I_{s,N} \tag{11}$$

It is worth to mention that the harmonic components of the back-emf, apart from the fundamental component, do not give any contribution to the active electric power when the current is sinusoidal but just determines the torque ripple of the PM BLDC motor, which is formulated in the next Subsection B.

By (3), (8) and (11), the nominal motor torque for sinusoidal current supply is given by

$$T_{s,N} = \frac{18k_\Phi}{\pi^2}I_{s,N} \tag{12}$$

and its p.u. expression becomes

This article has been accepted for publication in a future issue of this journal, but has not been fully edited. Content may change prior to final publication. Citation information: DOI 10.1109/TIE.2015.2455518, IEEE Transactions on Industrial Electronics

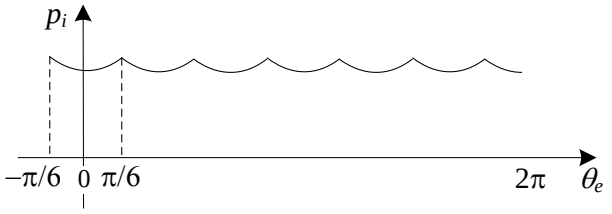

Fig.4. Instantaneous electric power as a function of the angular phase.

$$T_{s,N,pu} = \frac{18}{\sqrt{3}\pi^2} \cong 1.05 \tag{13}$$

Eq. (13) shows that i) the motor torque is constant from zero up to the base speed, which is determined in the next Subsection C, and ii) the nominal torque with sinusoidal current supply is 5% greater than with the ideal square-wave counterpart.

B. Torque ripple

From the trace of p_i, calculated according to (5) and plotted in Fig.4, it can be realized that i) the sinusoidal current supply produces a torque ripple that has a period of one sixth the supply period, i.e. of $\pi/3$, i) the torque ripple has an half-period symmetry, and iii) within the $\pi/3$ interval around the origin, the maximum torque occurs at $\theta = \pm \pi/6$ and the minimum torque at θ=0. Then the torque ripple for sinusoidal current supply of nominal magnitude results in

$$TR_{s,N} = \tau_{s,N}\left(\pm\frac{\pi}{6}\right) - \tau_{s,N}(0) \tag{14}$$

and, in p.u., it is expressed as

$$TR_{s,N,pu} = \left(\frac{2}{\sqrt{3}} - 1\right) \cong 0.155 \tag{15}$$

Note that $TR_{s,N}$ remains the same over the entire speed range up to the base speed.

A useful remark is about the torque at zero speed: as it emerges from Fig. 4, the motor torque depends on the position of the rotor whilst there is no torque ripple since the motor is at standstill. Therefore, even if it does not have a strict meaning, the motor torque and the torque ripple at zero speed can be defined respectively as the average value and the excursion of the torque for a span of the rotor position over an electrical angle of π/3.

C. Base speed

For sinusoidal current supply, the base speed is defined as the maximum speed at which the VSI is able to impress sinusoidal currents of nominal magnitude into the motor phases.

The motor phase voltage, f.i. across the phase *a*, is plotted in Fig.5. The line-to-line voltage v_{ab} of the motor, given by

$$v_{ab} = \underbrace{L\frac{d(i_a - i_b)}{dt}}_{v_{L,ab}} + \underbrace{e_a - e_b}_{e_{ab}} \tag{16}$$

is plotted in Fig.6. According to the trace, v_{ab} has an half-wave symmetry. Under nominal sinusoidal current, v_{ab} is expressed in the angular interval [0, π/6] as

$$v_{ab} = \sqrt{3}\,p\Omega L I_{s,N}\cos\left(\theta_e + \frac{\pi}{6}\right) + k_\Phi\Omega\left(1 + \frac{6}{\pi}\theta_e\right) \tag{17}$$

As shown in Appendix A, the derivative of (17) is always positive, provided that

$$\frac{4k_\Phi}{\pi p L I_{s,N}} > 1 \tag{18}$$

At nominal speed, the voltage drop on the phase inductance caused by the nominal current is $V_{L,N} = p\Omega_N L I_{s,N}$. Inequality (18) can be written as a function of $V_{L,N}$ and of $E_N = k_\Phi\Omega_N$ in the form

$$E_N > \frac{\pi}{4}V_{L,N} \tag{19}$$

Inequality (19) is well satisfied by the commercial PM BLDC motors, where the nominal back-emf is much larger than $V_{L,N}$. Further to (19), v_{ab} reaches the peak at $\theta_e = \pi/6$, and the peak magnitude is equal to

$$V_{ab,peak} = \frac{\sqrt{3}}{2}p\Omega L I_{s,N} + 2k_\Phi\Omega \tag{20}$$

In turn, the maximum magnitude of the line-to-line peak voltage generated by a VSI in the linear modulation zone is equal to the DC source voltage V_N. Then, equating $V_{ab,peak}$ to V_N and solving for Ω, it follows that the base speed for the sinusoidal supply is

$$\Omega_{s,B} = \frac{V_N}{2k_\Phi}\frac{1}{1 + \frac{\sqrt{3}}{2}\frac{pLI_{s,N}}{2k_\Phi}} \rightarrow \Omega_{s,B,pu} = \frac{1}{1+\Theta_m} \tag{21}$$

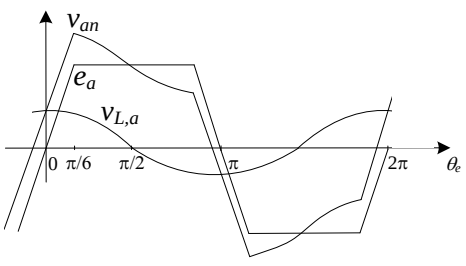

Fig.5. Phase voltage waveform

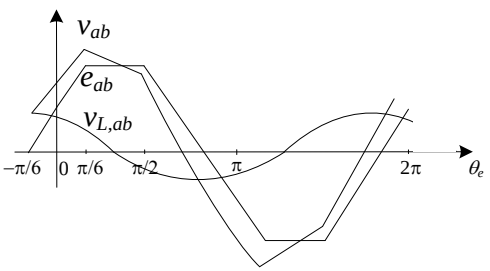

Fig.6. Line-to-line voltage waveform.

This article has been accepted for publication in a future issue of this journal, but has not been fully edited. Content may change prior to final publication. Citation information: DOI 10.1109/TIE.2015.2455518, IEEE Transactions on Industrial Electronics

In (21) the motor-specific parameter Θ_m is introduced; it is given by

$$\Theta_m \hat{=} \frac{\sqrt{3}}{2}\frac{pLI_{s,N}}{2k_\Phi} = \frac{pLI_N}{2k_\Phi} \tag{22}$$

where the last relationship descends from (8). Parameter Θ_m has the dimension of radians and takes a typical value of a few cents of radian for most PM BLDC motors. It plays a significant role with the real square-wave current supply in determining the current behavior during the commutations as well as the torque performance [9].

D. Voltage saturation operation

Beyond the base speed $\Omega_{s,B}$, the motor operates under voltage saturation. In this speed range, that goes from $\Omega_{s,B}$ to Ω_O, the magnitude of the sinusoidal current must be reduced for the VSI to operate in the linear modulation zone. Therefore, by (20), the peak magnitude of the current under voltage saturation turns out to be

$$I_{s,sat} = \frac{2}{\sqrt{3}}\frac{V_N - 2k_\Phi\Omega}{p\Omega L} \tag{23}$$

As demonstrated in Appendix B, the motor torque and the torque ripple, under voltage saturation and supply current magnitude in (23), become

$$T_{s,sat,pu} = \frac{18}{\sqrt{3}\pi^2\Theta_m}\frac{1-\Omega_{pu}}{\Omega_{pu}} \cong \frac{1.05}{\Theta_m}\frac{1-\Omega_{pu}}{\Omega_{pu}} \tag{24}$$

$$TR_{s,sat,pu} = \frac{\frac{2}{\sqrt{3}}-1}{\Theta_m}\frac{1-\Omega_{pu}}{\Omega_{pu}} \cong \frac{0.155}{\Theta_m}\frac{1-\Omega_{pu}}{\Omega_{pu}} \tag{25}$$

IV. Torque Performance Comparison

A. Real square-wave current supply

In this Subsection, the torque performance of a PM BLDC drive with real square-wave current supply is reminded. As documented in the literature [8], two different commutation processes occur depending on whether the motor speed is lower or greater than $\Omega_0/2$. As a matter of fact, in both the processes, during the first part of the commutation interval, all the three motor phases conduct because the phase current to be removed continues to circulate through the relevant free-wheeling diode. Instead, during the second part of the commutation interval that starts at the angle when one of the two commutating currents reaches first its final value, there is the transient of either the injected current to reach the required magnitude or the removed current to reach the zero value.

A close investigation of the characteristics of a PM BLDC drive produced by the commutation phenomenon is carried out in [9]. It shows that for the commutation process occurring at low speeds -denoted by the subscript ℓ-, the torque excursion during the commutations is positive and the motor torque exceeds, even if only a little, that one with the ideal square-wave current supply. Under nominal current, the motor torque is

$$T_{q,\ell,pu} = 1 + \frac{3\Theta_m}{2\pi}\frac{1-2\Omega_{pu}}{2-\Omega_{pu}} \tag{26}$$

and the torque ripple is

$$TR_{q,\ell,pu} = \frac{1-2\Omega_{pu}}{2-\Omega_{pu}} \tag{27}$$

Instead, for the commutation process occurring at high speeds -denoted with the subscript *h*-, the torque excursion during the commutations is negative and the motor torque is less than one with the ideal square-wave current supply. Under nominal current, the motor torque is

$$T_{q,h,pu} = 1 - \frac{3\Theta_m}{2\pi}\frac{(2\Omega_{pu}-1)\Omega_{pu}}{1-\Omega_{pu}^2} \tag{28}$$

and the torque ripple is

$$TR_{q,h,pu} = 1 - \frac{2-\Omega_{pu}}{1+\Omega_{pu}} \tag{29}$$

For the real square-wave current supply, the base speed $\Omega_{q,N}$ is defined as the maximum speed at which the VSI is able to bring the injected current at the nominal value I_N at least at half of the conduction interval of $2\pi/3$, where the successive commutation of a phase starts. It is

$$\Omega_{q,B,pu} = \frac{1}{1+\frac{3\Theta_m}{\pi}} \tag{30}$$

and the corresponding torque value is

$$T_{q,B,pu} = \frac{3}{2}\frac{1+\frac{3\Theta_m}{\pi}}{2+\frac{3\Theta_m}{\pi}} \tag{31}$$

Beyond the base speed, the motor operates under voltage saturation. In this speed range, that goes from $\Omega_{q,B}$ to Ω_O, the magnitude of the injected current is less than I_N even at half of the conduction interval, and the motor torque and the torque ripple are given by

$$T_{q,sat,pu} = \frac{\pi}{2\Theta_m}\frac{1-\Omega_{pu}}{\Omega_{pu}(1+\Omega_{pu})} \tag{32}$$

$$\Delta T_{q,sat,pu} = \frac{\pi}{3\Theta_m}\frac{(1-\Omega_{pu})(2\Omega_{pu}-1)}{\Omega_{pu}(1+\Omega_{pu})} \tag{33}$$

B. Convenience analysis

The p.u. motor torque and torque ripple for the sinusoidal and real square-wave supplies are plotted in Figs. 7 and 8, respectively. As a case study, the commercial PM BLDC

This article has been accepted for publication in a future issue of this journal, but has not been fully edited. Content may change prior to final publication. Citation information: DOI 10.1109/TIE.2015.2455518, IEEE Transactions on Industrial Electronics

drive with the data reported in Appendix C is used.

A cross-examination of the graphs shows the better performance of the sinusoidal current supply both from the point of view of the motor torque and the torque ripple. In addition to the already mentioned 5% greater value of the motor torque, the graphs of Fig. 7 together with the data reported in Tab. I, point out that i) the PM BLDC drive with sinusoidal current supply develops a constant torque up to the base speed while its real square-wave counterpart develops a torque that decreases starting from about half the base speed and becoming about 0.77 times lower than the nominal torque at the base speed, ii) the base speeds for the two types of current supply are almost equal, and iii) beyond the base speed, the torque of the PM BLDC drive decreases in a nearly linear way for both the current supplies.

Besides, the graphs of Fig. 8 point out that i) the torque ripple with sinusoidal current supply is constant from zero up to the base speed, while it varies with the real square-wave current supply; the reason is that the current waveform remains sinusoidal at any speed for the sinusoidal current supply while it changes with the speed during the commutations for the real square-wave current supply, and ii) the torque ripple with sinusoidal current supply is much lower both at low and high speeds while it exceeds the real square-wave current supply in a speed interval of about 0.22 p.u. centered at half of the nominal speed. This because around $\Omega_0/2$ the real square-wave current supply experiences an increase in the injected current that occurs at nearly the same rate as the decrease in the current to be removed, thus yielding a compensating action on the torque excursion [9].

A numerical computation has been executed to investigate the effect of the motor resistances on the speed-torque characteristics of the PM BLDC drive with the two types of current supply. The investigation has revealed that the voltage drop across the motor resistances reduces the base speed of about the same quantities for the two current supplies. To be more precise, the base speed reduction is 0.9 times the value reported in Tab. I for the sinusoidal current supply and about 0.89 times for the real square-wave current supply. This proves that the assumption of neglecting the voltage drop on motor resistances does not modified the above results substantially.

The traces of the instantaneous torque obtained by a computer-assisted analysis for the two types of current supply are plotted in Fig. 9 (a) and (b), respectively. The traces refer to a motor speed of about Ω_{pu}=0.8 (i.e. 575 rpm), and to the nominal current I_N (50 A) for the real square-wave current supply and $I_{s,N}$ (58 A) for the sinusoidal current supply. The motor torque is equal to 0.93 p.u. with the real square-wave supply while it reaches 1.04 p.u. with the sinusoidal current supply; both the values are in good agreement with the results of Fig. 7. Torque ripples, instead, are a few percent greater

TABLE I. PM BLDC DERIVED QUANTITIES

Data	Symbol	Value
Motor-specific parameter	Θ_m	46.8 mrad
Base speed with sinusoidal current supply	$\Omega_{s,B,pu}$	0.955
Base speed with square-wave current supply	$\Omega_{q,B,pu}$	0.957
Torque at base speed with square-wave current supply	$T_{q,B,pu}$	0.77

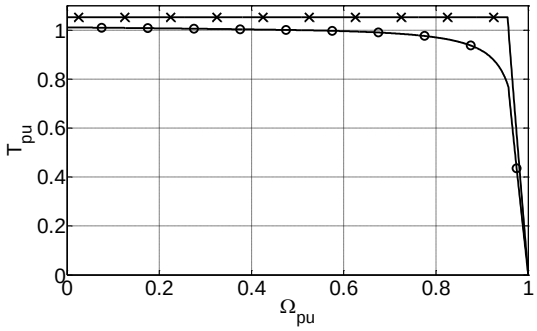

Fig.7. Per-unit torque-speed characteristic with sinusoidal current supply (x marks) and real square-wave current supply (o marks).

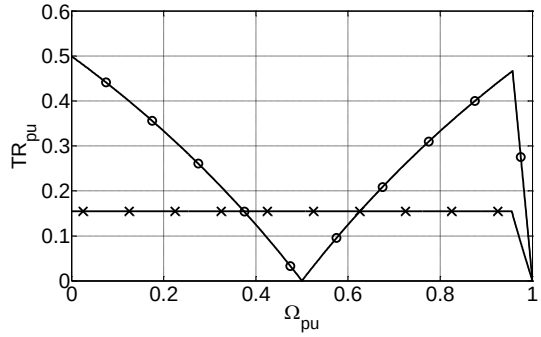

Fig.8. Per-unit torque ripple vs. speed with sinusoidal current supply (x marks) and real square-wave current supply (o marks).

than the results of Fig. 8 and are due to the torque harmonics produced by the high-frequency current harmonics ensuing from the PWM voltage supply. In any case, the torque ripple with the sinusoidal current supply is about half of the torque ripple with the real square-wave current supply, thus demonstrating the convenience of the sinusoidal current supply.

A question can arise about the behavior of an equivalent PM BLAC motor having a peak back-emf equal to that one of the PM BLDC motor and supplied with a sinusoidal current whose the rms value is equal to that one of the PM BLDC motor. As explained in [5], in nominal conditions the torque developed by the PM BLAC motor is 0.866 times less than the one of the PM BLDC motor; therefore it is about 20% less than the nominal torque of a PM BLDC motor with sinusoidal current supply. The trace of the instantaneous torque for the PM BLAC motor at about Ω_{pu}=0.8 is plotted in Fig. 9 (c). Like for the sinusoidal current supply, it exhibits a torque ripple produced by the high-frequency current harmonics ensuing from PWM voltage supply.

C. Efficiency

The efficiency of a PM DC motor can be expressed as

$$\eta_x = \frac{P_{x,m,pu} - P_{x,lm,pu}}{P_{x,m,pu} + P_{x,lB,pu} + P_{x,lCu,pu}} \tag{34}$$

where subscript x stands for q or s according to the current supply, $P_{x,m,pu}$ is the total electromagnetic power generated by the motor, $P_{x,lm,pu}$ are the mechanical power losses, $P_{x,lB,pu}$ are the magnetic power losses and $P_{x,lCu,pu}$ are the power losses in the phase resistances, all expressed in p.u.

To simplify the analysis, let us i) approximate the losses of the real square-wave current supply to the ones of the ideal square-wave supply, and ii) neglect the power losses $P_{x,lm,pu}$ and $P_{x,lB,pu}$.

This article has been accepted for publication in a future issue of this journal, but has not been fully edited. Content may change prior to final publication. Citation information: DOI 10.1109/TIE.2015.2455518, IEEE Transactions on Industrial Electronics

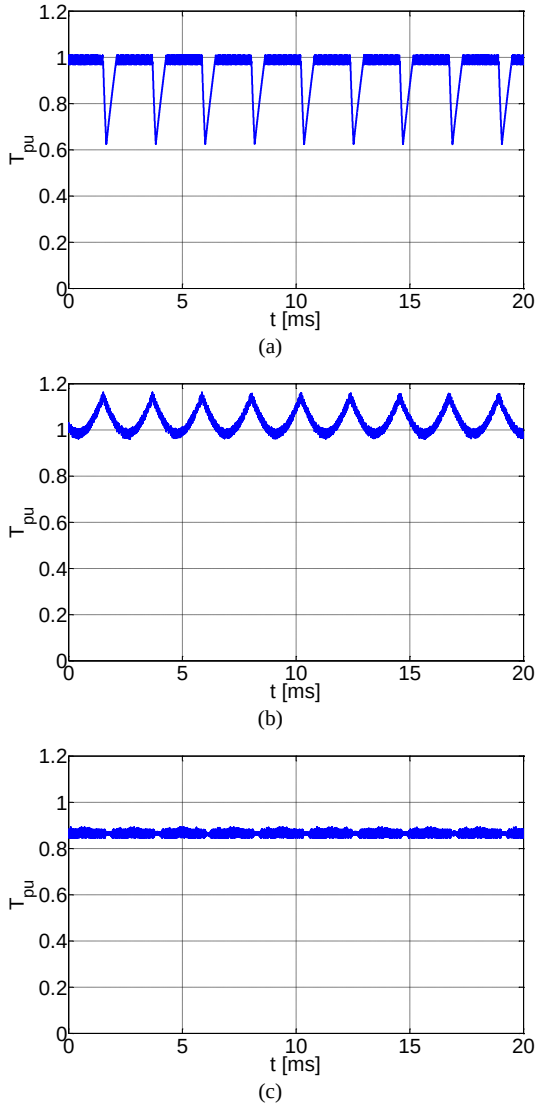

Fig.9. Instantaneous torque with (a) real square-wave current supply, (b) sinusoidal current supply, and (c) sinusoidal current supply of an equivalent PM BLAC motor.

For the square-wave current supply, $P_{q,m,pu}$ and $P_{q,lCu,pu}$ at nominal rms current are respectively given by

$$P_{q,m,pu} = \begin{cases} T_{q,\ell,pu}\Omega_{pu} & for\ \ \Omega_{pu} < 0.5 \\ T_{q,h,pu}\Omega_{pu} & for\ 0.5 < \Omega_{pu} < \Omega_{q,B,pu} \end{cases} \quad (35)$$

$$P_{q,lCu,pu} = \frac{3I_N^2 R}{2kI_N\Omega_N} = 3P_{R,pu} \quad (36)$$

For the sinusoidal current supply with an equal rms current, $P_{s,m,pu}$ is given by (37) while $P_{s,lCu,pu}$ has the same expression as $P_{q,lCu,pu}$.

$$P_{s,m,pu} = T_{s,N,pu}\Omega_{pu} \quad (37)$$

Then the efficiency for the two current supplies becomes

$$\eta_q = \begin{cases} \eta_{q,l} = \frac{T_{q,\ell,pu}\Omega_{pu}}{T_{q,\ell,pu}\Omega_{pu}+3P_{R,pu}} & for\ \ \Omega_{pu} < 0.5 \\ \eta_{q,h} = \frac{T_{q,h,pu}\Omega_{pu}}{T_{q,h,pu}\Omega_{pu}+3P_{R,pu}} & for\ 0.5 < \Omega_{pu} < \Omega_{q,B,pu} \end{cases} \quad (38)$$

$$\eta_s = \frac{T_{s,N,pu}\Omega_{pu}}{T_{s,N,pu}\Omega_{pu}+3P_{R,pu}} \quad (39)$$

and their ratio is

$$\frac{\eta_s}{\eta_q} = \begin{cases} \frac{T_{s,N,pu}}{T_{s,N,pu}\Omega_{pu}+3P_{R,pu}} \frac{T_{q,\ell,pu}\Omega_{pu}+3P_{R,pu}}{T_{q,\ell,pu}} & for\ \ \Omega_{pu} < 0.5 \\ \frac{T_{s,N,pu}}{T_{s,N,pu}\Omega_{pu}+3P_{R,pu}} \frac{T_{q,h,pu}\Omega_{pu}+3P_{R,pu}}{T_{q,h,pu}} & for\ 0.5 < \Omega_{pu} < \Omega_{q,B,pu} \end{cases} \quad (40)$$

At the two speeds Ω_{pu}=0.955 and Ω_{pu}=0.455 the efficiency ratios are

$$\frac{\eta_s}{\eta_q}(\Omega_{pu} = 0.955) = \frac{0.78+3.16P_{R,pu}}{0.78+2.34P_{R,pu}} \quad (41)$$

$$\frac{\eta_s}{\eta_q}(\Omega_{pu} = 0.455) = \frac{0.48+3.16P_{R,pu}}{0.48+3.00P_{R,pu}} \quad (42)$$

For the study case, $P_{R,pu}$ is calculated in 0.058; therefore (41) and (42) result in

$$\frac{\eta_s}{\eta_q}(\Omega_{pu} = 0.955) = 1.052 \quad (43)$$

$$\frac{\eta_s}{\eta_q}(\Omega_{pu} = 0.455) = 1.014 \quad (44)$$

Equations (43) show that at high speeds the efficiency of the motor supplied by sinusoidal current is a little greater than with the square-wave supply because $T_{s,N,pu}$ is higher of $T_{q,h,pu}$. However, this difference becomes smaller at low speeds since the torque developed with the square-wave supply increases to $T_{q,N,pu}$. Moreover, if $P_{x,lm,pu}$ and $P_{x,lB,pu}$ are taken into account, the ratio between the efficiencies becomes closer to unity even at high speeds because these losses have almost the same value for the two current supplies and their contribution reduces the effect of the difference between $T_{s,N,pu}$ and $T_{q,h,pu}$.

V. Experimentation

A. Experimental setup

The scheme of the experimental setup is drawn in Fig. 10. The control board is built up around the starter kit TMS320F28335 eZdsp, produced by Texas Instrument for its DSP F28335, and is entered by i) the signals coming from three Halls sensors, ii) the signal coming from two phase current sensors, and iii) the torque reference. The control scheme impresses into the motor sinusoidal currents in-phase with the back-emfs by operating in a d,q synchronous frame to reduce the phase shift between reference and actual currents. The angle selected for the transformation is the angular phase θ_e of the back-emf of the phase *a* and is estimated with the block denoted as "transformation angle estimator" by means of the algorithm described in the following Subsection.

The torque reference τ_{ref} ranges from zero to the nominal value in (13) in the constant torque region and from zero to the value in (24) in the voltage-saturated region to keep the VSI in the linear modulation zone. From τ_{ref}, the reference $i_{d,s,ref}$ of the d-axis current can be readily obtained from (12) as

$$i_{d,s,ref} = \frac{\pi^2}{18k_\Phi}\tau_{ref} \quad (45)$$

Note that, as a consequence of the angle selected for the transformation and the current and back-emf traces in Fig.3,

This article has been accepted for publication in a future issue of this journal, but has not been fully edited. Content may change prior to final publication. Citation information: DOI 10.1109/TIE.2015.2455518, IEEE Transactions on Industrial Electronics

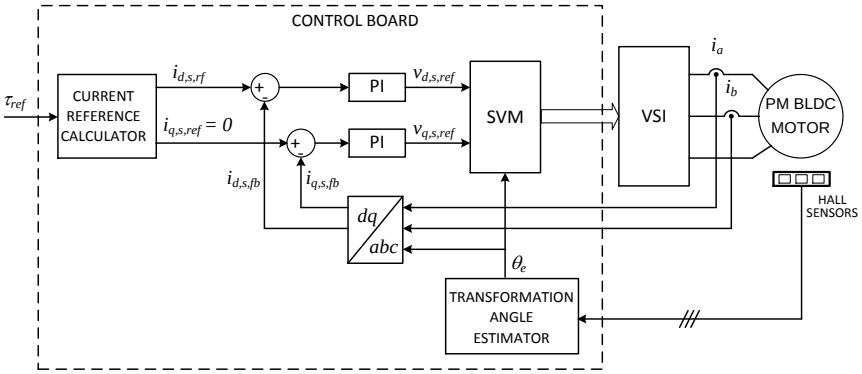

Fig.10. Sinusoidal current supply scheme.

the torque-component of the current is here given by its d-axis projection. Under the hypothesis that the *d,q* transformation is amplitude-invariant, (45) coincides with the reference of the peak value of the sinusoidal supply currents. Since no current is requested along the q-axis, the reference $i_{q,s,ref}$ is set at 0.

The two current references are compared to the relevant feedbacks $i_{d,s,fb}$ and $i_{q,s,fb}$. The differences are processed by PI regulators to generate the voltage references $v_{d,s,ref}$ and $v_{q,s,ref}$ in the synchronous frame, which are then entered together with θ_e into the space vector modulation (SVM) block to generate the PWM commands for the VSI.

Current regulators have been designed by imposing a control loop bandwidth of 1 kHz with a phase margin of 90°. Conventional method based on the Bode diagrams has been used to find out the regulator parameters; then the transfer function of the controllers has been discretized using the Euler method and implemented in the firmware of the control board.

In the experimental setup the load torque is applied to the PM BLDC motor by help of an ancillary speed-controlled PM BLAC drive whose motor is engaged to the motor of the PM BLDC drive through a gear. Speed and torque feedback signals of the auxiliary drive are read and referred to the speed and torque of the PM BLDC drive by respectively dividing and multiplying the read values by the gear ratio.

B. Angular phase estimation

If the angular phase should be determined by detecting the edges of the Hall signals, it would have a resolution of $\pi/3$ radians. Such a resolution is not enough for an accurate processing in the *d,q* synchronous frame of the sinusoidal currents that must supply the motor. To overcome this problem and, at the same time, to avoid the usage of an absolute encoder that would be much more expensive than the Hall sensors, the angular phase θ_e is estimated by the following algorithm:

$$\theta_e(k) = \theta_e(k-1) + \Omega_e \Delta t \qquad (46)$$

where Δt is the sampling period, set equal to half of the PWM period, *k* is the sampling time, and Ω_e is calculated as the ratio of $\pi/3$ to the time length of the interval between the two previously detected edges of the Hall signals. Such a way of calculating Ω_e is fair since the motor speed does not change appreciably from a two-edge interval to the successive one if the interval is enough short, i.e. if the motor speed is not too much small. The experiments have shown that the speed accuracy is good for Ω greater than about 10% of its nominal value Ω_N. To comply with this condition, the firmware developed for the experimental setup starts the motor with a square-wave current supply and automatically jumps to the sinusoidal current supply when the calculated value of Ω exceeds $0.1\Omega_N$.

C. Experimental results

At first, correct functioning of the supply scheme has been verified at various motor speed. For instance, the traces of the phase currents for the motor rotating at a speed of about 0.28 and 0.90 p.u. are plotted in Figs. 11 (a) and (b), respectively. The first current trace refers to the PM BLDC drive operating in the constant torque region at the nominal current whilst the second one refers to the drive operating in the voltage-saturated region at about half the nominal current. Note that distortion of the sinusoidal current and PWM oscillations are appreciable in the voltage-saturated region since the voltage drops due to the phase resistance and the VSI leg dead-time become significant compared to the voltage required to win the phase back-emf and inductance voltage drop. As a comparison, Fig. 11 (c) reports the trace of the phase current for the motor rotating at the speed of 0.82 p.u., which is a little less than the nominal one, under real square-wave current supply and nominal current reference. The trace shows that i) at the injection, the current takes a long time to increase and -furthermore- does not reach the nominal value, ii) at the removal, the current takes a short time to vanish, iii) at the commutation of the other two phases, the current exhibits an appreciable negative excursion, and iv) as a result, the trace makes evident one more time the torque drop at high speeds.

Next, the torque-speed characteristic of the PM BLDC drive is found by measuring the torque developed by the motor at different speeds. With the view to find it correctly, a preliminary set of tests have been executed to determine the friction torque of the experimental setup. To this purpose, the PM BLDC motor has been disconnected from the VSI and the torque exerted by the ancillary drive to rotate the PM BLDC motor has been measured for different speeds. The friction torque helps braking the drive under test and hence it has been added to the torque exerted by the ancillary drive to obtain the total torque developed by the PM BLDC drive. The resulting torque-speed characteristic of the PM BLDC drive with the sinusoidal current supply is reported in Fig. 12 both

This article has been accepted for publication in a future issue of this journal, but has not been fully edited. Content may change prior to final publication. Citation information: DOI 10.1109/TIE.2015.2455518, IEEE Transactions on Industrial Electronics

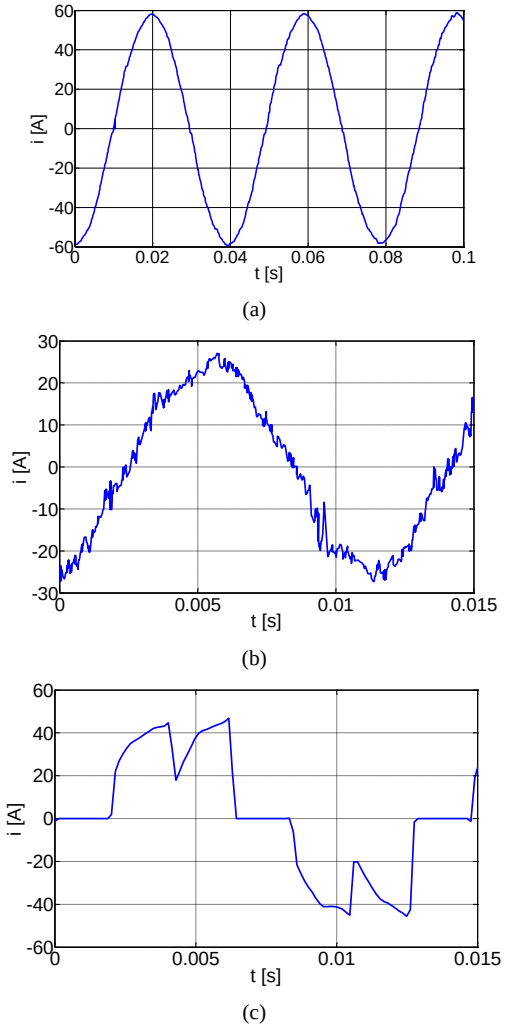

Fig.11. (a) Current waveform with sinusoidal current supply at (a) 0.28, (b) 0.90, and c) current waveform with the real square-wave supply at 0.82. Speeds are given in p.u.

in the constant-torque and voltage-limited region. In the same figure, the resulting torque-speed characteristic of the same PM BLDC drive with the real square-wave current supply are also reported with the stars. The experimental results fully agree with the theoretical findings, and demonstrate the overall superior torque performance achievable with the sinusoidal current supply.

VI. Conclusions

The paper has formulated the torque performance of a PM BLDC drive with sinusoidal current supply, in terms of torque-speed characteristic, torque ripple and base speed. Afterwards, it has compared the resulting performance with that one of the drive when supplied with real square-wave currents. The theoretical results, corroborated by experiments, have demonstrated that the sinusoidal current supply outperforms the real square-wave current supply almost all over the speed range. Indeed, the torque-speed characteristic is higher, especially when approaching the base speed, and the torque ripple is lower, apart from a speed interval centered at half of the nominal speed and long about 22% of the nominal speed.

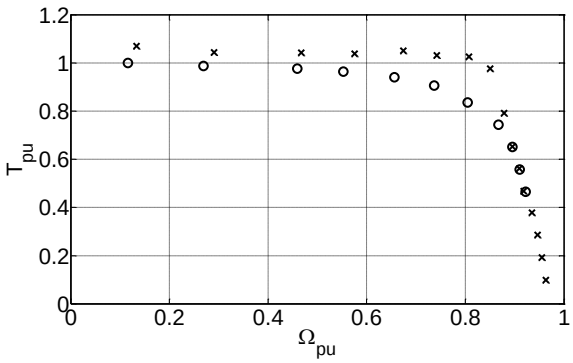

Fig.12. Torque-speed characteristics for sinusoidal (x marks) and real square-wave (o marks) current supplies.

Appendices

A. *Derivative of the phase-to-phase voltage v_{ab}*

Derivative of (17), given by

$$\frac{dv_{ab}}{d\theta_e} = -\sqrt{3}\,p\Omega L I_{s,N}\,sin\left(\theta_e + \frac{\pi}{6}\right) + \frac{6k_\Phi\Omega}{\pi} \tag{A.1}$$

is positive if

$$\frac{6k_\Phi}{\pi\sqrt{3}\,pLI_{s,N}} > sin\left(\theta_e + \frac{\pi}{6}\right) \tag{A.2}$$

In the angular interval [0, π/6] it is

$$\frac{1}{2} \le sin\left(\theta_e + \frac{\pi}{6}\right) \le \frac{\sqrt{3}}{2} \tag{A.3}$$

By (A.3), inequality (A.2) is surely fulfilled if the term on the right hand-side is higher than $\sqrt{3}/2$. This leads to (18).

B. *Torque under voltage saturation with sinusoidal current supply*

The expression of the torque generated by PM BLDC drive with sinusoidal current supply while operating in voltage saturation is derived from (12) and (23) by replacing $I_{s,N}$ with $I_{s,sat}$, and results in

$$T_{s,sat} = \frac{18\times 2k_\Phi}{\sqrt{3}\pi^2}\,\frac{V_N - 2k_\Phi\Omega}{p\Omega L} \tag{A.4}$$

Eq. (A.4) can be rearranged as in (A.5) in order to express $T_{s,sat}$ as a function of the parameter Θ_m defined in (22) and of T_N. Then $T_{s,sat,pu}$ can be expressed as in (A.6).

$$T_{s,sat} = \frac{18\times 2k_\Phi}{\sqrt{3}\pi^2}\,\frac{T_N}{pLI_N}\,\frac{V_N - 2k_\Phi\Omega}{2k_\Phi\Omega} \tag{A.5}$$

$$T_{s,sat,pu} = \frac{18}{\sqrt{3}\pi^2}\,\frac{1}{\Theta_m}\left(\frac{V_N}{2k_\Phi\Omega} - 1\right) \tag{A.6}$$

Finally, by expressing in (A.6) the speed Ω in p.u., (24) is obtained. Eq. (25) can be obtained in a similar way.

This article has been accepted for publication in a future issue of this journal, but has not been fully edited. Content may change prior to final publication. Citation information: DOI 10.1109/TIE.2015.2455518, IEEE Transactions on Industrial Electronics

C. Study case PM BLDC drive

A commercial PM BLDC drive manufactured by the H.T.M. Company has been used as a study case. The motor is designed for the in-wheel propulsion of light electric vehicles. The drive comes with a three-phase MOSFET VSI commanded with a PWM frequency of 14 kHz. Rated values and measured parameters of the motor are listed in Tab. II.

TABLE II. PM BLDC DRIVE DATA.

Data	Symbol	Value
Nominal motor voltage	V_N	48 V
Nominal motor current	I_N	50 A
Conventional nominal motor speed	Ω_N	640 rpm
Phase resistance (inclusive of the transistor on-resistance)	R	50 mΩ
Inclusive phase inductance	L	75 μH
Motor constant	k_Φ	0.32 V·s/rad
Pole pairs	p	8
Rated torque	T_N	32 N·m
Peak torque	T_P	100 N·m

REFERENCES

[1] B.K. Bose, "*Power electronics and motor drives: advances and trends*", Elsevier-Academic Press, 2006.

[2] T.J.E.Miller, "*Brushless permanent-magnet and reluctance motor Drives*", Clarendon Press, Oxford 1989.

[3] P.Pillay and K.Ramu, "Application characteristics of permanent magnet synchronous and brushless DC motors for servo drives", *IEEE Trans. Ind. Applic.*, vol. 27, no. 5, pp. 986-996, September/October 1991.

[4] K.T.Chau, C.C.Chan, and C.Liu, "Overview of permanent-magnet brushless drives for electric and hybrid electric vehicles," *IEEE Trans. Ind. Electron.*, vol. 55, no. 6, pp. 2246-2257, 2008.

[5] K.Ramu, "*Permanent magnet synchronous motors and brushless DC motor drives*", Taylor & Francis, CRC Press, Boca Raton, 2010.

[6] J.De la Ree, "Performance evaluation of PM machines with quasi-square input currents", *Electric Machines & Power Systems*, vol. 18, n° 3, pp. 283-291, 1990.

[7] B.H.Kang, C.J.Kim, H.S.Mok, and G.H.Choe, "Analysis of torque ripple in BLDC motor with commutation time", in *Proc. of IEEE Intern. Symp. on Ind. Electron., (ISIE)* 2001, vol. 2, pp. 1044-1048.

[8] R.Carlson, M.Lajoie-Mazenc, and J.C. dos S.Fagundes, "Analysis of torque ripple due to phase commutation in brushless DC machine", *IEEE Trans. Ind. Applic.*, vol.28, no.3, pp.632-638, May/June 1992.

[9] M.Bertoluzzo, G.Buja, R.K.Keshri, and R.Menis, "Analytical study of torque vs. speed characteristics of PM brushless DC drives", in *Proc. of 38th IEEE Annual Conf. of the Ind. Electron. Soc. (IECON)*, 2012, pp. 1684-1689.

[10] Y. Liu, Z.Q. Zhu, and D. Howe, "Direct torque control of brushless DC drives with reduced torque ripple," *IEEE Trans. Ind. Applic.*, vol. 41, no. 2, pp. 599-607, Mar./Apr. 2005.

[11] C. Xia, Y. Xiao, W. Chen, and T. Shi, "Torque ripple reduction in brushless DC drives based on reference current optimization using integral variable structure control," *IEEE Trans. Ind. Electron.*, vol. 61, no. 2, pp. 738-752, 2014.

[12] S.J.Park, H.W.Park, M.H.Lee, and F.Harashima, "A new approach for minimum-torque-ripple maximum-efficiency control of BLDC motor," *IEEE Trans. Ind. Electron.*, vol. 47, no. 1, pp. 109-114, Feb. 2000.

[13] C.Xia, Y.Wang, and T.Shi, "Implementation of finite-state model predictive control for commutation torque ripple minimization of permanent-magnet brushless DC motor", *IEEE Trans. Ind. Electron.*, vol. 60, no. 3, pp. 896-905, March 2013.

[14] H.Le-Huy, R.Perret, and R.Feuillet, "Minimization of Torque Ripple in Brushless DC Motor Drives", *IEEE Trans. on Ind. Applic.*, Vol.IA-22, NO. 4, pp. 748-755, July/August 1986.

[15] S.B.Ozturk and H.A.Toliyat, "Direct Torque control of brushless dc motor with non-sinusoidal back-EMF", in *Proc. of IEEE Int. Electric Machines and Drives Conf. (IEMDC)*, 2007, Vol. 1, pp. 165-171.

[16] S.B.Ozturk and H.A.Toliyat, "Direct Torque and Indirect Flux Control of Brushless DC Motor", *IEEE/ASME Trans. Mech.*, Vol. 16, No. 2, pp. 351-360, April 2011.

[17] M.S.Islam, S.Mir, T.Sebastian and S.Underwood, "Design considerations of sinusoidally excited permanent magnet machines for low torque ripple applications", in *Proc. of 39th IEEE Annual Meeting of the Ind. Applic. Soc. (IAS)*, 2004, pp. 1723-1730.

[18] R.Somanatham, P.V.N.Prasad, and A.D.Rajkumar, "Simulation of PMBLDC motor with sinusoidal excitation using trapezoidal control strategy," in *Proc. of 1st IEEE Conf. on Ind. Electron and Applic. (ICIEA)*, 2006, pp.1-6.

[19] S.Wang, "BLDC ripple torque reduction via modified sinusoidal PWM" in *Proc. in Fairchild Semiconductor Power Seminar* 2008-2009, pp.1-10.

Manuele Bertoluzzo received the M.S. degree in electronic engineering and the Ph.D. degree in industrial electronics and computer science from the University of Padova, Padova, Italy, in 1993 and 1997, respectively. From 1998 to 2000, he was a member of the Research and Development Division of an electric drive factory. In 2000, he joined the Department of Electrical Engineering, University of Padova, as a Researcher in the Scientific Disciplines' Group "electric converters, machines, and drives." He holds the temporary lectureship of Enertronics for graduate students. He is currently involved in the analysis and design of power electronics and control systems for purely and hybrid vehicles.

Giuseppe Buja (M'75–SM'84–F'95-LF'13) is a Full Professor at the University of Padova, Italy, with classes on Electric systems for automation and Electric road vehicles. He has carried out research in the field of power and industrial electronics and has authored or co-authored more than 200 papers published in refereed international journals and conference proceedings. His current research is turned to the electric vehicles, included wired and wireless charging equipment, and to power systems for renewable energies. He was the recipient of the IEEE Industrial Electronics Society Eugene Mittelmann Achievement Award "in recognition of his outstanding technical contributions to the field of industrial electronics". Dr. Buja has served the IEEE in several capacities, including General Chairman of the 20th Annual Conference of Industrial Electronics. Presently, he is a senior member of the Administrative Committee of IES society and a member of a number of scientific associations and conference committees.

Ritesh Kumar Keshri (M'08–SM'15), received B.Sc (Engg.) and M.Tech from National Institute of Technology, Jamshedpur, India, in 2003 and 2007 respectively both in electrical engineering and PhD from Department of Industrial Engineering (DII) University of Padova (UniPD), Italy in March 2014. Since 2006 he is with Department of Electrical and Electronic Engineering, BIT Mesra, India as an Assistant Professor. Mr. Keshri received silver medal for being first in M. Tech (electrical) in 2007, Young researcher fellowship from Ministry of University of Italy in 2008, Erasmus Mundus Fellowship for 34 months, from European Union in 2010, and won first prize as a student team leader of the University of Padova in class-3 of Formula Electric and Hybrid in 2011. His research interests include power electronics and electric drives for electric vehicle propulsion.

Roberto Menis (M'91) was born in Osoppo (Udine), Italy. He is Associate Professor of Electric Drives at the Department of Engineering and Architecture of the University of Trieste, he is the head of the Electric Drives Laboratory and coordinator of the Master Degree Course in Electrical Energy and Systems Engineering. His fields of interest are modeling and parameter identification of ac machines; control of ac motors; industry and transport applications of the electric drives; dependability and functional safety applied to the electrical systems for transportations (automotive and naval areas).